Biogeosciences Discuss., 10, 17397–17438, 2013
www.biogeosciences-discuss.net/10/17397/2013/
doi:10.5194/bgd-10-17397-2013

Biogeosciences Discussions
Open Access

Methane and nitrous oxide fluxes from the tropical Andes

Y. A. Teh[1,*], T. Diem[1], S. Jones[2], L. P. Huaraca Quispe[3], E. Baggs[4], N. Morley[4], M. Richards[4], P. Smith[4], and P. Meir[2,5]

[1]Department of Earth and Environmental Sciences, University of St Andrews, Scotland, UK
[2]School of Geosciences, University of Edinburgh, Scotland, UK
[3]Universidad Nacional de San Antonio Abad del Cusco, Peru
[4]Institute of Biological and Environmental Sciences, University of Aberdeen, Scotland, UK
[5]Research School of Biology, Australian National University, Canberra, Australia
[*]now at: Institute of Biological and Environmental Sciences, University of Aberdeen, Cruickshank Building, St Machar Drive, Aberdeen, AB24 3UU, Scotland, UK

Received: 30 September 2013 – Accepted: 14 October 2013 – Published: 5 November 2013

Correspondence to: Y. A. Teh (yateh@abdn.ac.uk)

Published by Copernicus Publications on behalf of the European Geosciences Union.

Abstract

Remote sensing and inverse modelling studies indicate that the tropics emit more CH_4 and N_2O than predicted by bottom-up emissions inventories, suggesting that terrestrial sources are stronger or more numerous than previously thought. Tropical uplands are a potentially large and important source of CH_4 and N_2O often overlooked by past empirical and modelling studies. To address this knowledge gap, we investigated spatial, temporal and environmental trends in CH_4 and N_2O fluxes across a long elevation gradient (600–3700 m a.s.l.) in the Kosñipata Valley, in the southern Peruvian Andes that experiences seasonal fluctuations in rainfall. The aim of this work was to produce preliminary estimates of CH_4 and N_2O fluxes from representative habitats within this region, and to identify the proximate controls on soil CH_4 and N_2O dynamics. Ecosystems across this altitudinal gradient were both atmospheric sources and sinks of CH_4 on an annual basis. Montane grasslands (or, puna; 3200–3700 m a.s.l.) were strong atmospheric sources, emitting 56.94 ± 7.81 kg $CH_4 - C$ ha^{-1} yr^{-1}. Upper montane forest (2200–3200 m a.s.l.) and lower montane forest (1200–2200 m a.s.l.) were net atmospheric sinks (-2.99 ± 0.29 kg $CH_4 - C$ ha^{-1} yr^{-1} and -2.34 ± 0.29 kg $CH_4 - C$ ha^{-1} yr^{-1}, respectively); while premontane forests (600–1200 m a.s.l.) fluctuated between source or sink depending on the season (wet season: 1.86 ± 1.50 kg $CH_4 - C$ ha^{-1} yr^{-1}; dry season: -1.17 ± 0.40 kg $CH_4 - C$ ha^{-1} yr^{-1}). Analysis of spatial, temporal and environmental trends in CH_4 flux across the study site suggest that soil redox was a dominant control on net CH_4 flux. CH_4 emissions were greatest from elevations, landforms and during times of year when soils were sub-oxic, and CH_4 efflux was inversely correlated with soil O_2 concentration ($r^2 = 0.82$, $F_{1,125} = 588.41$, $P < 0.0001$). Ecosystems across the region were net atmospheric N_2O sources. N_2O fluxes declined with increasing elevation; N_2O emissions from premontane forest, lower montane forest, upper montane forest and montane grasslands averaged 2.23 ± 1.31 kg $N_2O - N$ ha^{-1} yr^{-1}, 1.68 ± 0.44 kg $N_2O - N$ ha^{-1} yr^{-1}, 0.44 ± 0.47 kg $N_2O - N$ ha^{-1} yr^{-1} and 0.15 ± 1.10 kg $N_2O - N$ ha^{-1} yr^{-1}, respectively. N_2O fluxes from premontane and lower montane forests exceeded prior

BGD
10, 17397–17438, 2013

model predictions for the region. Comprehensive investigation of field and laboratory data collected in this study suggest that N_2O fluxes from this region were primarily driven by denitrification; that nitrate (NO_3^-) availability was the principal constraint on N_2O fluxes; and that soil moisture and water-filled porosity played a secondary role in modulating N_2O emissions. Any current and future changes in N management or anthropogenic N deposition may cause shifts in net N_2O fluxes from these tropical montane ecosystems, further enhancing this emission source.

1 Introduction

Recent remote sensing and inverse modelling studies indicate that the tropics emit more methane (CH_4) and nitrous oxide (N_2O) than estimated from prior bottom-up emissions inventories, suggesting that tropical sources are stronger or more numerous than previously thought (Frankenberg et al., 2005, 2008; Bergamaschi et al., 2009; Fletcher et al., 2004a, b; Hirsch et al., 2006; Huang et al., 2008; Kort et al., 2011). Recent speculation over discrepancies in the global tropical CH_4 budget have focussed on the potential role of seasonally flooded wetlands (Melack et al., 2004; Bergamaschi et al., 2009) or vegetation in accounting for budgetary gaps; the latter acting either as abiotic producers (Bergamaschi et al., 2007) or conduits for atmospheric egress from anoxic soils (Gauci et al., 2010; Terazawa et al., 2007). Parallel debates over tropical N_2O budgets have invoked rising agricultural emissions or atmospheric transport processes as possible causes for discrepancies between top-down and bottom-up budgets (Nevison et al., 2007, 2011; Kort et al., 2011).

One potentially important source of CH_4 and N_2O overlooked both by bottom-up inventories or top-down studies are fluxes from tropical uplands (Spahni et al., 2011), because attention has historically focussed on seasonally inundated wetlands (e.g. *várzea* in Brazil) (Fung et al., 1991; Bergamaschi et al., 2009; Melack et al., 2004; Werner et al., 2007), lowland forests, savannas, or pastures (Hall and Matson, 1999; Silver et al., 1999; Teh et al., 2005; Werner et al., 2007; Keller et al., 1986, 1993;

BGD
10, 17397–17438, 2013

Verchot et al., 2000; Keller and Reiners, 1994). However, upland ecosystems account for a substantial fraction of land cover in the tropics; in South America alone, upland ecosystems (> 500 m a.s.l.) represent more than 8 % of total continental land cover (Eva et al., 2004), while in mountainous countries, such as Peru or other Andean states, upland ecosystems may account for upwards of 80 % of total land cover (Feeley and Silman, 2010). Measurements from tropical uplands in Australia (Breuer et al., 2000), Ecuador (Wolf et al., 2011, 2012), Hawaii (Hall and Matson, 1999, von Fischer and Hedin, 2002, 2007), Puerto Rico (Silver et al., 1999; Teh et al., 2005) and Sulawesi (Veldkamp et al., 2008; Purbopuspito et al., 2006) indicate that CH_4 and N_2O fluxes from these environments are comparable or greater than those from tropical lowlands, and may therefore be quantitatively important in regional and global atmospheric budgets, particularly if these ecosystems function as regional "hotspots" of gas production or consumption (Teh et al., 2011; Waddington and Roulet, 1996). CH_4 fluxes in tropical uplands are particularly intriguing because they show no clear regional patterns or trends; while some ecosystems function as net atmospheric sources, others operate as net atmospheric sinks (Wolf et al., 2011, 2012; Silver et al., 1999; Teh et al., 2005, von Fischer and Hedin, 2002; Veldkamp et al., 2008). N_2O fluxes are more predictable but are still poorly constrained (Werner et al., 2007); upland ecosystems, like their lowland counterparts, act as net N_2O sources, with emission rates modulated by factors such as soil moisture, water-filled pore space, soil oxygen content, redox potential, C availability, inorganic N availability (NH_4^+, NO_3^-), or competition for NO_3^- among different soil sinks (Hall and Matson, 1999; Silver et al., 1999, 2001; Veldkamp et al., 2008; Wolf et al., 2011, 2012; Firestone and Davidson, 1989).

In the Neotropics, data on upland CH_4 and N_2O fluxes are particularly scarce, with field observations only from Puerto Rico (Silver et al., 1999; Teh et al., 2005) and Ecuador (Wolf et al., 2011, 2012). Because of the limited spatial coverage and aseasonality of these two regions, it is difficult to draw wider conclusions about the source or sink strength of Neotropical uplands for CH_4 and N_2O, particularly for areas that experience marked seasonality in rainfall or temperature. To address these knowledge

BGD
10, 17397–17438, 2013

gaps, we performed a preliminary study of CH_4 and N_2O cycling across a long elevation gradient (600–3700 m a.s.l.) in the Peruvian Andes that experiences seasonal variations in rainfall, and include a wide range of habitats stretching from premontane forests to wet montane grasslands. Our principal objectives were to:

1. Quantify spatial (elevation, topography or landform) and temporal (seasonal, month-to-month) trends in CH_4 and N_2O fluxes
2. Evaluate the role of environmental variables in modulating CH_4 and N_2O dynamics

Findings from this research will provide the basis for future more detailed and integrative studies of soil trace gas dynamics in seasonal montane tropical ecosystems; and will also enable us to identify the proximate controls on CH_4 and N_2O fluxes in these diverse environments.

2 Methods and materials

2.1 Study site

Measurements were conducted on the eastern slope of the Andes in the Kosñipata Valley, Manu National Park, Peru (Malhi et al., 2010). This 3.02×10^6 ha (30 200 km^2) region has been the subject of intensive ecological, biogeochemical and climatological studies since 2003 by the Andes Biodiversity and Ecosystem Research Group (or, ABERG; http://www.andesconservation.org), and contains a series of long-term permanent plots across a 200–3700 m a.s.l. elevation gradient stretching from the western Amazon to the Andes (Malhi et al., 2010; Feeley and Silman, 2010). This part of the Andes experiences pronounced seasonality in rainfall but not in air temperature; the dry season extends from May to September and the wet season from October to April (Girardin et al., 2010; Zimmermann et al., 2010a). Thirteen sampling plots (approximately 20 m × 20 m each) were established at four different elevations across a gradi-

BGD
10, 17397–17438, 2013

ent spanning 600–3700 m a.s.l., including premontane forest (600–1200 m a.s.l.; $n = 3$ plots), lower montane forest (1200–2200 m a.s.l.; $n = 3$ plots), upper montane forest (2200–3200 m a.s.l.; $n = 3$ plots), and montane grasslands (3200–3700 m a.s.l.; $n = 4$ plots; hereafter referred to as "puna"). In premontane forest, new sampling plots were established in Hacienda Villa Carmen, a 3,065 ha biological reserve operated by the Amazon Conservation Association (ACA), containing a mixture of old-growth forest, secondary forest and agricultural plots. Sampling for gas fluxes was concentrated in the old-growth portions of the reserve. For lower montane and upper montane forests, sampling plots were established adjacent to or within existing 1 ha permanent sampling plots established by ABERG. New sampling plots were also established in puna to capture a representative range of environmental conditions, microforms (1–5 m scale landforms) and mesotopes (100 m–1 km scale landforms) (Belyea and Baird, 2006), as past ABERG studies of puna biogeochemistry were more limited in spatial extent (Gibbon et al., 2010; Zimmermann et al., 2010b). Mesotopic features include ridges, slopes, flats and basins. The latter two landforms include wet, grassy lawns with no discernible grade; and peat-filled depressions found in valley bottoms, respectively. Some (although not all) of these basins abut pool or lake complexes. Because of the logistic challenges of sampling over open water, we did not collect data from the pools or lakes, nor from the shoreline. Summary site descriptions are provided in Table 1 with data on site characteristics collated from prior studies (Feeley and Silman, 2010; Girardin et al., 2010; Zimmermann et al., 2009, 2010b).

2.2 Soil–atmosphere exchange

Field sampling was performed over a 13 month period from December 2010 to December 2011 for all habitats except premontane forest. Because of circumstances outside our control, only 6 months of data were collected for premontane forest, with sampling only commencing in July 2011. Soil–atmosphere fluxes were collected monthly, except where flooding or landslides prevented safe access by fieldworkers to the study sites. Gas exchange rates were determined with five replicate gas flux chambers deployed in

BGD
10, 17397–17438, 2013

each of the thirteen plots (n = 65 flux observations per month). Sampling was spatially stratified to account for mesotope (100 m–1 km) scale variability in redox and hydrologic conditions (Belyea and Baird, 2006); key environmental factors that often regulate soil–atmosphere trace gas fluxes (Silver et al., 1999; Teh et al., 2011). All representative landforms were sampled in each elevation band, including ridges, slopes, flats and basins (Table 1). This spatial stratification of sampling was justified by a prior pilot study conducted across the entire ABERG elevation gradient (i.e. 220–3700 m a.s.l.), which found significant within and among plot variability in fluxes, suggesting the need for a spatially explicit sampling design (Saiz and Teh, 2009, unpublished data; n = 75 static chamber measurements; > 10 flux measurements per elevation).

Daily sampling in puna for 12 days (from 11 November 2011 to 22 November 2011) was performed in order to determine if CH_4 and other trace gas fluxes varied among mesotope-scale landforms (ridge, slope, flat, basin) in response to short-term (daily) fluctuations in rainfall, water table depth and soil moisture content. Sampling followed a stratified design that encompassed a 2.5 ha area including ridge, slope, flat and basin landforms. Twenty-four sampling stations were set-up across this topographic gradient > 1 month prior to sampling, consisting of six 75 m long transects, each running perpendicular to the slope and containing 4 sampling stations each. Each sampling station was instrumented with a chamber base, a soil gas equilibration chamber buried at a depth of 10 cm (Teh et al., 2005), and a piezometer inserted to bedrock or saprolite depth (≤ 50 cm). Measurements of air temperature, flux chamber temperature, soil temperature (5 and 10 cm depth), atmospheric pressure, soil moisture (0–20 cm), soil oxygen (O_2) concentration and water table depth were collected concurrent with flux chamber measurements on a daily basis.

Soil–atmosphere fluxes of CH_4, N_2O and CO_2 were determined using a static flux chamber approach (Teh et al., 2011; Livingston and Hutchinson, 1995), although only CH_4 and N_2O fluxes are reported here. Static flux chamber measurements were made by enclosing a 0.03 m^2 area with cylindrical, opaque (i.e. dark), two-component (i.e. base and lid) vented chambers. Chamber bases were permanently installed to a depth

BGD
10, 17397–17438, 2013

of approximately 5 cm and inserted > 1 month prior to the commencement of sampling, in order to avoid potential artefacts from root mortality following base emplacement (Varner et al., 2003). Chamber lids were fitted with small computer case fans to promote even mixing in the chamber headspace (Pumpanen et al., 2004). Headspace samples were collected from each flux chamber over a 30 min enclosure period, with samples collected at 4 discrete intervals using a gastight syringe. Gas samples were stored in evacuated Exetainers® (Labco Ltd., Lampeter, UK), shipped to the UK by courier, and subsequently analysed for CH_4, N_2O and CO_2 concentrations using a Thermo TRACE GC Ultra (Thermo Fisher Scientific Inc., Waltham, Massachusetts, USA) at the University of St Andrews. Chromatographic separation was achieved using a Porapak-Q column, and analyte concentrations quantified using a flame ionization detector (FID) for CH_4, electron capture detector (ECD) for N_2O, and methanizer-FID for CO_2. Instrumental precision was determined by repeated analysis of standards and was better than 5 % for all detectors. Fluxes rates were determined by using the R (R Core Team, 2012) HMR package to plot best-fit lines to the data for headspace concentration against time for individual flux chambers (Pedersen et al., 2010). Gas mixing ratios (ppm) were converted to areal fluxes by using the Ideal Gas Law to solve for the quantity of gas in the headspace (on a mole or mass basis), normalized by the surface area of each static flux chamber (Livingston and Hutchinson, 1995).

2.3 Environmental variables

To investigate the effects of environmental variables on trace gas dynamics, we determined soil moisture, soil oxygen content in the 0–10 cm depth, soil temperature, chamber temperature and air temperature at the time of flux sampling. In flooded environments (e.g. puna basins), water table depth was also measured using piezometers installed to a depth of ≤ 50 cm in the soil. Soil moisture was determined using portable moisture probes (ML2x ThetaProbe, Delta-T Device Ltd., Cambridge, UK) inserted into the substrate immediately adjacent to each flux chamber (< 5 cm from each chamber base; depth of 0–10 cm). Soil moisture content was measured both as volumetric wa-

BGD
10, 17397–17438, 2013

ter content (VWC) and water-filled pore space (WFPS), the latter calculated from VWC and bulk density data (Breuer et al., 2000). Soil O_2 concentration was determined by analysing soil gas with a portable O_2 meter (Apogee Instruments Ltd., Logan, Utah, USA), collected from soil gas equilibration chambers permanently installed to a depth of 0–10 cm adjacent to static flux chambers (Teh et al., 2005). Soil temperature (0–10 cm depth), chamber temperature and air temperature was determined using type K thermocouples (Omega Engineering Ltd., Manchester, UK). Data on aboveground litterfall, meteorological variables (i.e. photosynthetically active radiation, air temperature, relative humidity, rainfall, wind speed, wind direction), continuous plot-level soil moisture and soil temperature measurements (10 cm and 30 cm depths) were also collected, but are not reported in this publication.

Fluctuations in available inorganic N (i.e. ammonium, NH_4^+; nitrate, NO_3^-; nitrite, NO_2^-) concentrations were quantified in all plots using a resin bag approach (Templer et al., 2005). From August 2011 onwards, ion exchange resin bags ($n = 15$ resin bags per elevation) were deployed in the rhizosphere (i.e. 0–10 cm depth in premontane forest, lower montane forest and puna; 0–15 cm in upper montane forest), and collected at monthly intervals (where possible) for determination of monthly time-averaged NH_4^+, NO_3^- and NO_2^- concentrations. For some plots, this sampling frequency was periodically disrupted due to natural hazards (i.e. land slides, river flooding) preventing safe access to the study sites. Resin bags were shipped to the University of Aberdeen after collection from the field, inorganic N was extracted using 2 N KCl (Templer et al., 2005) and concentrations determined colorimetrically using a Burkard SFA2 continuous-flow analyzer (Burkard Scientific Ltd., Uxbridge, UK).

2.4 Denitrification potentials and N_2O yields

Potential denitrification rates across the elevation sequence were determined by performing an exploratory ^{15}N-labeled nitrate (^{15}N-NO_3^-) laboratory tracer study (Baggs et al., 2003; Bateman and Baggs, 2005). Details of the soil sampling scheme for this experiment are summarised in Table 2. Twenty-two soils samples (125–170 g dry soil

BGD
10, 17397–17438, 2013

per sample) were collected from beneath the rooting zone from sites across the elevation sequence, air-dried and then shipped to the UK by courier. Upon arrival in the UK, 50 g dry soil sub-samples were taken from each soil sample and weighed out into 52 700 mL glass vessels for incubation ($n = 19$ for premontane forest, $n = 3$ for lower montane forest, $n = 5$ for upper montane forest, $n = 10$ for puna). The uneven sample sizes reflect the fact that this experiment was designed as a preliminary scoping exercise to capture a broad range of environmental conditions, microtopographic and mesotopic features in order to quantify the range of variability in denitrification rates both within and among elevation bands. Soil sub-samples were initially re-wetted to 20 % volumetric water content, and allowed to pre-incubate for 4 days. Soils were further moistened at the start of the experiment to achieve a final WFPS of 80 %. A KNO_3 solution containing 0.2 mL of 0.01 M 40 atom % $^{15}N\text{-}NO_3^-$ was then added to the soil, and the glass incubation vessels sealed to initiate the experiment. Control incubations were conducted with soils from each elevation band ($n = 3$ per elevation) to correct for the ^{15}N natural abundance signature of endogenous N_2O and N_2 production. Gas samples were collected at 0, 6, 12, 24, 33 and 48 h to quantify N_2O, $^{15}N\text{-}N_2O$ and $^{15}N\text{-}N_2$ concentrations. Gas concentrations and isotope ratios were determined at the University of Aberdeen, using an Agilent 6890 GC fitted with an ECD (Agilent Technologies UK Ltd., Workingham, UK) and a SerCon 20 : 20 isotope ratio mass spectrometer (IRMS) equipped with an ANCA TGII pre-concentration module (SerCon Ltd., Crewe, UK), respectively. Instrumental precision was determined by repeated analysis of standards and was better than 5 % for both the GC and IRMS. Potential denitrification rates were calculated from the difference in the ^{15}N atom % excess values of N_2O and N_2 relative to the controls. Fluxes of $^{15}N\text{-}N_2O$ and $^{15}N\text{-}N_2$ were determined using the R (R Core Team; http://www.r-project.org) HMR package (as described above) and normalized for soil dry weight. Total denitrification potential (i.e. sum of $^{15}N\text{-}N_2O$ plus $^{15}N\text{-}N_2$ fluxes) and N_2O yield (i.e. the ratio of $^{15}N\text{-}N_2O : {}^{15}N\text{-}N_2O$ flux + $^{15}N\text{-}N_2$ flux) were also calculated (Yang et al., 2011).

BGD
10, 17397–17438, 2013

2.5 Statistical analyses

Statistical analyses were performed using JMP IN Version 8 (SAS Institute, Inc., Cary, North Carolina, USA) and R (R Core Team, 2012). The data were log transformed where necessary to meet the assumptions of analysis of variance. Residuals were checked for heteroscedasticity and homogeneity of variances. Repeated measures analysis of variance (ANOVA) was used to explore the influence of spatial (e.g. elevation band, topography) and temporal factors (e.g. day of year, season) on gas fluxes and environmental variables. A student's *t* test was used to compare differences in fluxes and environmental variables between seasons (dry, wet). Bivariate or multiple regression was utilized to investigate the relationship among environmental variables and trace gas fluxes. Repeated measures analysis of covariance (ANCOVA) was used to evaluate the relative contribution of ordinal variables (elevation band, topography, day of year, season) and continuous environmental covariates (soil moisture, soil oxygen, soil temperature, air temperature) in regulating gas fluxes. Means comparisons were performed using Fisher's Least Significant Difference test (Fisher's LSD). Statistical significance was determined at the $P < 0.05$ level, unless otherwise noted. Values are reported as means and standard errors (±1 SE).

3 Results

3.1 Spatial variation in gas fluxes and environmental variables

The mean CH_4 flux for the entire 13 month dataset was $7.79 \pm 1.14\,mg\,CH_4 - C\,m^{-2}\,d^{-1}$. CH_4 fluxes varied significantly among elevation bands (habitats) and over time (repeated measures ANOVA, $r^2 = 0.91$, $F_{101,731} = 75.75$, $P < 0.00001$). Multiple comparisons tests indicated that CH_4 fluxes from puna differed significantly from other habitats (Fisher's LSD, $P < 0.05$; Fig. 1a). Puna were net sources of CH_4, with mean fluxes of $15.60 \pm 2.14\,mg\,CH_4 - C\,m^{-2}\,d^{-1}$. In contrast, premontane, lower montane and upper

BGD
10, 17397–17438, 2013

montane forests were all net atmospheric sinks, with mean uptake rates of $-0.16 \pm 0.13\,mg\,CH_4 - C\,m^{-2}\,d^{-1}$, $-0.64 \pm 0.08\,mg\,CH_4 - C\,m^{-2}\,d^{-1}$ and $-0.82 \pm 0.08\,mg\,CH_4 - C\,m^{-2}\,d^{-1}$, respectively (Fig. 1a). CH_4 fluxes varied significantly among topographic features (ANOVA, $r^2 = 0.54$, $F_{6,826} = 161.15$, $P < 0.0001$; data not shown). Basin landforms, found only in the puna, emitted significantly more CH_4 than other topographic features (mean CH_4flux for basin landforms was $63.99 \pm 7.80\,mg\,CH_4 - C\,m^{-2}\,d^{-1}$; Fisher's LSD, $P < 0.05$; data not shown). Other landforms were either weak sources or sinks, but could not be distinguished from each other statistically because of the large variance in fluxes. The mean for pooled CH_4 fluxes from ridge, slope and flat landforms (i.e. the entire dataset excluding basin landforms) was $0.47 \pm 0.18\,mg\,CH_4 - C\,m^{-2}\,d^{-1}$, with a range from -8.71 to $78.5\,mg\,CH_4 - C\,m^{-2}\,d^{-1}$.

The mean N_2O flux for the entire 13 month dataset was $0.22 \pm 0.12\,mg\,N_2O - N\,m^{-2}\,d^{-1}$. N_2O fluxes varied widely among elevations bands (habitats) and over time (repeated measures ANOVA, $r^2 = 0.17$, $F_{76,381} = 1.06$, $P < 0.35$). Mean N_2O fluxes declined progressively with increasing elevation, although this pattern was only statistically significant at the $P < 0.1$ level due to high variance in fluxes both within and among study sites (Fig. 1b). The highest mean fluxes observed were in premontane forests ($0.61 \pm 0.36\,mg\,N_2O - N\,m^{-2}\,d^{-1}$), followed by lower montane forests ($0.46 \pm 0.12\,mg\,N_2O - N\,m^{-2}\,d^{-1}$), upper montane forests ($0.12 \pm 0.13\,mg\,N_2O - N\,m^{-2}\,d^{-1}$) and puna ($0.04 \pm 0.30\,mg\,N_2O - N\,m^{-2}\,d^{-1}$) (Fig. 1b). N_2O fluxes did not vary significantly among topographic features within elevation bands (ANOVA, $r^2 = 0.02$, $F_{6,451} = 1.36$, $P > 0.2$).

Soil moisture varied significantly among elevation bands (habitats) and over time. Patterns were qualitatively similar whether volumetric water content or WFPS were used as metrics of soil moisture (repeated measures ANOVA for VWC, $r^2 = 0.86$, $F_{104,800} = 46.42$, $P < 0.0001$; repeated measures ANOVA for WFPS, $r^2 = 0.72$, $F_{76,628} = 18.57$, $P < 0.0001$). Multiple comparison tests indicate that soil moisture varied significantly among elevations (Fisher's LSD, $P < 0.05$; Table 3). Soil moisture

BGD
10, 17397–17438, 2013

was greatest in puna (VWC: 72.9 ± 0.2 %; WFPS: 94.7 ± 0.3 %) followed by premontane forest (VWC: 42.0 ± 1.4 %; WFPS: 70.1 ± 2.3 %). Lower montane forest (VWC: 35.0 ± 0.7 %; WFPS: 58.4 ± 1.2 %) and upper montane forest (VWC: 31.9 ± 0.9 %; WFPS: 58.0 ± 1.6 %) had significantly lower levels of soil moisture than either puna or premontane forest. Soil moisture varied significantly among topographic features (ANOVA for VWC, $r^2 = 0.70$, $F_{6,898} = 350.76$, $P < 0.0001$; ANOVA for WFPS, $r^2 = 0.42$, $F_{6,622} = 73.62$, $P < 0.0001$). Soil moisture patterns among topographic features varied depending on elevation band. For example, soil moisture did not vary significantly among landforms in premontane forest. In contrast, in lower montane forest, ridges and slopes were not statistically different from each other (ridge: VWC: 35.5 ± 1.3 %, WFPS: 59.1 ± 2.2 % and slope: VWC: 38.4 ± 1.5 %, WFPS: 64.1 ± 2.5 %), but were significantly wetter than flat areas (VWC: 31.4 ± 0.8 %, WFPS: 57.4 ± 1.4 %). For upper montane forest, ridges were significantly wetter than slopes (ridge: VWC: 37.0 ± 1.5 %, WFPS: 67.3 ± 2.7 % versus slope: VWC: 38.4 ± 1.5 %, WFPS: 64.1 ± 2.5 %). For puna, soil moisture was highest in basins (VWC: 80.1 ± 0.8 %, WFPS: 97.5 ± 0.2 %), followed by flat areas and slopes (flat: VWC: 70.9 ± 0.7 %, WFPS: 94.7 ± 0.5 %; slope: VWC: 69.0 ± 0.6 %, WFPS: 95.1 ± 0.3 %), and driest on ridges (VWC: 68.2 ± 0.6 %, WFPS: 93.2 ± 0.6 %)

Soil O_2 concentrations in the 0–10 cm soil depth varied significantly among elevation bands (habitats) and over time (repeated measures ANOVA, $r^2 = 0.88$, $F_{48,269} = 40.08$, $P > 0.0001$). Multiple comparisons tests indicated that soil O_2 concentration in puna was significantly lower from that in other habitats (Fisher's LSD, $P < 0.05$; Table 3), with a mean value of 13.8 ± 0.3 %. Mean O_2 concentrations in premontane, lower montane and upper montane forests were 18.7 ± 0.3 %, 19.2 ± 0.1 % and 18.4 ± 0.1 %, respectively. Soil O_2 varied significantly among topographic features (ANOVA, $r^2 = 0.54$, $F_{6,594} = 118.58$, $P < 0.0001$); basin features showed significantly lower O_2 than other landforms (5.3 ± 0.9 %; Fisher's LSD, $P < 0.05$), but other topographic features did not differ significantly in O_2 concentration in the 0–10 cm soil depth. The pooled mean O_2

BGD
10, 17397–17438, 2013

concentration for ridge, slope and flat landforms was 17.1 ± 0.2 %, with a range from 0–21 % O_2.

Soil and air temperature varied significantly among elevation bands (habitats) and over time (repeated measures ANOVA for soil temperature, $r^2 = 0.83$, $F_{103,770} = 37.92$, $P < 0.0001$; repeated measures ANOVA for air temperature, $r^2 = 0.81$, $F_{75,492} = 28.50$, $P < 0.0001$). Multiple comparisons tests indicated that soil and air temperature were significantly different for each habitat (Table 3), with temperatures becoming progressively cooler with increasing elevation (Fisher's LSD, $P < 0.05$). Temperatures were highest in premontane forest (soil: 21.2 ± 0.1 °C; air: 23.4 ± 0.4 °C), followed by lower montane forest (soil: 18.1 ± 0.1 °C; air: 18.2 ± 0.1 °C), upper montane forest (soil: 11.8 ± 0.0 °C; air: 13.0 ± 0.1 °C) and puna (soil: 10.1 ± 0.1 °C; air: 11.8 ± 0.2 °C).

Available ammonium (NH_4^+) or nitrate (NO_3^-) concentrations varied significantly among elevation bands (habitats) and over time (repeated measures ANOVA for NH_4^+, $r^2 = 0.47$, $F_{60,151} = 2.22$, $P < 0.0001$; repeated measures ANOVA for NO_3^-, $r^2 = 0.81$, $F_{60,149} = 4.50$, $P < 0.0001$). In contrast, available NO_2^- concentrations varied widely among habitats and over time, but with no clear spatial or temporal trends (repeated measures ANOVA, $r^2 = 0.39$, $F_{60,154} = 1.61$, $P < 0.01$). For NH_4^+, multiple comparisons tests indicate that NH_4^+ concentration was greatest for upper montane forest, while other habitats did not differ significantly from each other (Fisher's LSD, $P < 0.05$; Fig. 2a). NH_4^+ concentration for the upper montane forest averaged 17.62 ± 1.33 μg NH_4^+ – N g resin^{-1} d^{-1}; in contrast, NH_4^+ concentrations from premontane forest, lower montane forest and puna averaged 12.28 ± 0.73 μg NH_4^+ – N g resin^{-1} d^{-1}, 14.82 ± 0.90 μg NH_4^+ – N g resin^{-1} d^{-1} and 12.78 ± 0.62 μg NH_4^+ – N g resin^{-1} d^{-1}, respectively. For NO_3^-, multiple comparisons tests indicate that NO_3^- concentrations decreased significantly with increasing elevation (Fisher's LSD, $P < 0.05$; Fig. 2b). Mean NO_3^- concentrations for premontane forest, lower montane forest, upper montane forest and puna were 17.67 ± 1.70 μg NO_3^- – N g resin^{-1} d^{-1}, 12.38 ± 1.87 μg NO_3^- – N g resin^{-1} d^{-1}, 4.92 ± 1.57 μg NO_3^- – N g resin^{-1} d^{-1} and 0.17 ± 0.02 μg NO_3^- – N g resin^{-1} d^{-1}, respec-

BGD
10, 17397–17438, 2013

tively. Available NO_2^- concentrations did not vary significantly among elevation bands, averaging $0.02 \pm 0.00\,\mu g\,NO_2^- - N\,g\,resin^{-1}\,d^{-1}$ across the elevation gradient (data not shown).

3.2 Temporal variability in gas exchange

CH_4 efflux increased during the wet season (repeated measures ANOVA, $r^2 = 0.91$, $F_{101,731} = 75.75$, $P < 0.00001$; Table 4), although there were no clear directional trends in fluxes within seasons. Furthermore, daily sampling in puna from 11 November 2011 to 22 November 2011 identified no apparent trends in CH_4 fluxes at this sampling frequency. Mean CH_4 fluxes in puna rose by a factor of 19 from dry season to wet season, from $0.97 \pm 0.47\,mg\,CH_4 - C\,m^{-2}\,d^{-1}$ in the dry season to $18.57 \pm 2.55\,mg\,CH_4 - C\,m^{-2}\,d^{-1}$ ($t_{431} = 4.01$, $P < 0.0001$). Net CH_4 uptake fluxes declined significantly from dry season to wet season for premontane, lower montane and upper montane forests (Table 4); the pooled mean dry season flux for the 3 forest types was $-0.86 \pm 0.05\,mg\,CH_4 - C\,m^{-2}\,d^{-1}$, while the pooled mean wet season flux was $-0.47 \pm 0.08\,mg\,CH_4 - C\,m^{-2}\,d^{-1}$ ($t_{398} = 4.08$, $P < 0.0001$). This pattern was most pronounced for premontane forest ($t_{49} = 2.76$, $P < 0.008$), where the direction of the soil–atmosphere flux was reversed from a weak atmospheric sink in the dry season ($-0.32 \pm 0.11\,mg\,CH_4 - C\,m^{-2}\,d^{-1}$) to a net atmospheric source during the wet season ($0.51 \pm 0.41\,mg\,CH_4 - C\,m^{-2}\,d^{-1}$).

N_2O fluxes across the elevation gradient showed no easily identifiable temporal trends. There was insufficient data to fully characterise seasonal trends in NH_4^+, NO_3^- and NO_2^- concentrations as only 4 months of data were collected over the sampling period. However, significant month-to-month variability was observed in NH_4^+, NO_3^- and NO_2^- concentrations.

BGD
10, 17397–17438, 2013

3.3 Temporal variability in environmental variables

Across the elevation gradient, soil moisture changed significantly over time, with temporal trends that varied depending on elevation band (repeated measures ANOVA for VWC, $r^2 = 0.86$, $F_{104,800} = 46.42$, $P < 0.0001$; repeated measures ANOVA for WFPS, $r^2 = 0.72$, $F_{76,628} = 18.57$, $P < 0.0001$). Soil moisture in premontane forest and puna showed significant month-to-month variability, but did not differ significantly between seasons (Table 3). In contrast, soil moisture in lower montane and upper montane forest rose significantly from dry season to wet season, with upper montane forest showing a more pronounced shift in soil water content (lower montane forest: VWC $t_{181} = 3.83$, $P < 0.0002$, dry season: 31.8 ± 1.0 %, wet season: 37.2 ± 1.0 %; upper montane forest: $t_{187} = 12.31$, $P < 0.05$, dry season: 22.7 ± 1.0 %, wet season: 37.7 ± 1.0 %).

Soil O_2 concentrations varied significantly over time, but temporal patterns differed for each elevation band (repeated measures ANOVA, $r^2 = 0.88$, $F_{48,269} = 40.08$, $P > 0.0001$). For lower montane forests, soil O_2 varied significantly from month-to-month, with small but statistically higher soil O_2 observed in the wet season (19.4 ± 0.1 %) compared to the dry season (19.0 ± 0.1 %) ($t_{90} = 3.21$, $P < 0.0002$; Table 3). Upper montane forests showed significant month-to-month variability, but no significant differences between seasons (overall mean = 18.4 ± 0.1 %). Puna showed a different trend from the other habitats, as lower O_2 concentrations were observed during the wet season (13.3 ± 0.4 %) compared to the dry season (18.4 ± 0.1 %) ($t_{379} = -3.48$, $P < 0.0006$; Table 3). Data on soil O_2 content in the premontane forest site was too sparse to evaluate seasonal patterns in soil O_2 content due to unanticipated delays in the installation of soil gas sampling equipment.

Soil temperature and air temperature varied significantly over time (repeated measures ANOVA for soil temperature, $r^2 = 0.83$, $F_{103,770} = 37.92$, $P < 0.0001$; repeated measures ANOVA for air temperature, $r^2 = 0.81$, $F_{75,492} = 28.50$, $P < 0.0001$). In premontane, lower montane and upper montane forests, the overall trend was towards significantly warmer soil and air temperatures forests during the wet season (Table 3).

BGD
10, 17397–17438, 2013

Puna showed a different pattern from the other study sites; no significant seasonal differences in soil temperature were observed, while air temperatures were warmer in the dry season (12.5 ± 0.3 °C) compared to the wet season (11.3 ± 0.2 °C) ($t_{198} = -3.53$, $P < 0.0005$; Table 3).

3.4 Relationships between gas fluxes and environmental variables

CH_4 fluxes across the elevation gradient were weakly correlated with soil moisture content (plot-averaged VWC versus CH_4 flux: $r^2 = 0.24$, $F_{1,152} = 48.64$, $P < 0.0001$; data not shown) and strongly negatively correlated with soil O_2 (plot-averaged soil oxygen versus CH_4 flux: $r^2 = 0.82$, $F_{1,125} = 588.41$, $P < 0.0001$; Fig. 3). A multiple regression model incorporating soil moisture and soil O_2 concentration explained only a further 1 % of the variance in the entire CH_4 dataset ($r^2 = 0.83$, $F_{2,124} = 295.47$, $P < 0.0001$), with soil O_2 accounting for > 99 % of the sum of squares in the multiple regression model (data not shown). No relationship between net CH_4 flux and temperature was found.

When these CH_4 flux data were disaggregated by elevation band and season, other relationships emerged, suggesting more habitat-specific controls on CH_4 flux. For lower montane forest, CH_4 fluxes were negatively correlated with soil temperature during the dry season (plot-averaged soil temperature versus CH_4 flux: $r^2 = 0.46$, $F_{1,13} = 10.86$, $P < 0.006$; data not shown), but not during the wet season. For puna, CH_4 fluxes were more strongly correlated with soil moisture content than for the overall pooled dataset ($r^2 = 0.24$ for the data pooled across the entire elevation gradient; data not shown). For example, taking both dry and wet season together for puna, the r^2 for the regression of CH_4 flux and VWC was 0.39 ($F_{1,64} = 41.44$, $P < 0.0001$), while the r^2 for the wet season data alone was higher ($r^2 = 0.46$, $F_{1,43} = 36.29$, $P < 0.0001$). Dry season puna CH_4 fluxes were not significantly correlated with VWC.

Only dry season N_2O fluxes from lower montane forest showed any relationship with environmental variables (Fig. 4), with N_2O fluxes negatively correlated with soil

BGD
10, 17397–17438, 2013

moisture content and WFPS (plot-averaged VWC or WFPS versus N_2O flux: $r^2 = 0.44$, $F_{1,9} = 7.10$, $P < 0.05$ for both VWC and WFPS, respectively). No other trends were found for other habitats or seasons, whether these data were pooled across the entire elevation gradient, or disaggregated by elevation band and season. There were insufficient data on NH_4^+, NO_3^- and NO_2^- concentrations to statistically determine if inorganic N fluxes were directly linked to N_2O emissions.

3.5 Denitrification potentials and N_2O yields

Analysis of variance indicated that $^{15}N\text{-}N_2O$ and $^{15}N\text{-}N_2$fluxes varied significantly among elevation bands (ANOVA for N_2O: $F_{3,33} = 4.42$, $P < 0.01$; ANOVA for N_2: $F_{3,33} = 2.89$, $P < 0.05$). Premontane forest, lower montane forest and puna showed similar rates of $^{15}N\text{-}N_2O$ and $^{15}N\text{-}N_2$flux (Fig. 5), with pooled means $^{15}N\text{-}N_2O$ and $^{15}N\text{-}N_2$ fluxes of $134.21 \pm 25.69\,\mu g\,N_2O - {}^{15}N\,kg\,soil^{-1}\,h^{-1}$ and $6.55 \pm 1.30\,\mu g\,N_2 - {}^{15}N\,kg\,soil^{-1}\,h^{-1}$, respectively. In contrast, upper montane forest showed significantly lower $^{15}N\text{-}N_2O$ flux ($7.39 \pm 7.33\,\mu g\,N_2O - {}^{15}N\,kg\,soil^{-1}\,h^{-1}$; Fisher's LSD, $P < 0.05$) and significantly greater $^{15}N\text{-}N_2$flux ($20.45 \pm 5.66\,\mu g\,N_2 - {}^{15}N\,kg\,soil^{-1}\,h^{-1}$; Fisher's LSD, $P < 0.05$).

Total denitrification potential did not vary significantly across elevation bands (ANOVA $F_{3,33} = 2.00$, $P > 0.13$; Fig. 5) due to high levels of variance in the component N_2O and N_2 fluxes. However, the overall trend was of lower total denitrification potential in the upper montane forest ($27.85 \pm 5.30\,\mu g\,^{15}N\,kg\,soil^{-1}\,h^{-1}$), whereas the other elevation bands showed similar total denitrification potentials (pooled mean of $140.75 \pm 25.97\,\mu g\,^{15}N\,kg\,soil^{-1}\,h^{-1}$). N_2O yields (i.e. ratio of $^{15}N\text{-}N_2O : {}^{15}N\text{-}N_2O$ flux + $^{15}N\text{-}N_2$ flux) varied significantly among elevation bands (ANOVA $F_{3,33} = 4.61$, $P > 0.01$; data not shown). Premontane, lower montane and puna had statistically similar N_2O yields (pooled mean of 0.79 ± 0.36), whereas upper montane forest showed the lowest N_2O yield overall (0.18 ± 0.40, Fisher's LSD, $P < 0.05$).

BGD
10, 17397–17438, 2013

4 Discussion

4.1 Andean ecosystems as both atmospheric sources and sinks of CH_4

Ecosystems across this tropical elevation gradient functioned as both atmospheric sources and sinks of CH_4, further challenging the long-standing assumption that tropical uplands are only net atmospheric CH_4 sinks (Dutaur and Verchot, 2007; Potter et al., 1996; Ridgwell et al., 1999; Teh et al., 2005, von Fischer and Hedin, 2002). CH_4 fluxes varied depending on elevation, topographic position and season. Montane grasslands (puna; 3200–3700 m a.s.l.) were net atmospheric sources; upper montane and lower montane forests were net sinks; and premontane forests fluctuated between sources or sinks depending on the season. From 600 to 3200 m a.s.l., the sink strength for atmospheric CH_4 increased with elevation. This pattern runs counter to observations from elsewhere in Latin America, such as Puerto Rico or Ecuador, where net CH_4 uptake decreased with increasing elevation (Silver et al., 1999; Teh et al., 2005; Wolf et al., 2012). The divergence between this study and others is likely due to local and regional differences in precipitation and soil moisture retention. Rainfall and soil moisture content decreases with rising elevation in this part of the Andes (Girardin et al., 2010), with the notable exception of puna, where soil moisture is elevated relative to other habitats across this elevation gradient due to poor drainage. In contrast, because of regional differences in climate and meteorology, soil moisture increases with elevation in Puerto Rico and Ecuador, favouring greater soil anaerobiosis, enhanced methanogenesis and diminished methanotrophy with rising altitude (Silver et al., 1999; Teh et al., 2005; Wolf et al., 2012).

CH_4 fluxes within elevation bands varied with topographic position, with lower topographic positions (e.g. basins) emitting more CH_4 than higher topographic positions (e.g. ridges). The development of more sub-oxic conditions in lower topographic positions likely drives greater methanogenesis and reduced methanotrophy; a common pattern observed in many other CH_4-emitting ecosystems (Teh et al., 2011; von Fischer et al., 2010; Waddington and Roulet, 1996; Silver et al., 1999). Across the entire

BGD
10, 17397–17438, 2013

altitudinal gradient, puna basins emitted more CH_4 than any other landform, releasing $233.56 \pm 28.47\,kg\,CH_4 - C\,ha^{-1}\,yr^{-1}$. Our findings are in general agreement with studies in Puerto Rico, where higher net CH_4 fluxes were observed from low topographic positions (Silver et al., 1999); but differ from research in Ecuador, where no significant difference was found in net CH_4 fluxes among topographic positions within an altitudinal band (Wolf et al., 2012). The most likely explanation for this divergence between the Peruvian and Puerto Rican transects on one hand, and the Ecuadorian transect on the other, is that the investigators in the latter study sampled only ridge and slope landforms, and did not sample lower topographic features such as flats or basins (Wolf et al., 2012). In addition, Wolf et al. (2012) did not sample more water-saturated puna habitats. Lower topographic landforms and puna habitats tend to accumulate water and contain more reduced soils capable of emitting CH_4, unlike more aerobic ridges and slopes that drain more freely (Teh et al., 2011; von Fischer et al., 2010; Waddington and Roulet, 1996; Silver et al., 1999).

CH_4 fluxes varied substantially depending on season, with an overall shift towards greater CH_4 emission or significant weakening of net soil sinks during the rainy season. These patterns were most pronounced for puna and premontane forest; the former showed a nineteen-fold increase in net CH_4 efflux from dry season to wet ($0.97 \pm 0.47\,mg\,CH_4 - C\,m^{-2}\,d^{-1}$ to $18.57 \pm 2.55\,mg\,CH_4 - C\,m^{-2}\,d^{-1}$), while the latter switched from a net atmospheric sink ($-0.32 \pm 0.11\,mg\,CH_4 - C\,m^{-2}\,d^{-1}$) to a net atmospheric source ($0.51 \pm 0.41\,mg\,CH_4 - C\,m^{-2}\,d^{-1}$). These seasonal trends differ significantly from Puerto Rico or Ecuador, where soil CH_4 fluxes did not vary on an intra-annual basis, presumably because of weaker rainfall seasonality in these other regions (Silver et al., 1999; Teh et al., 2005; Wolf et al., 2012). However, these data are consistent with findings from other seasonally dry tropical ecosystems, where greater net CH_4 efflux is associated with wetter periods of the year, where soil anaerobiosis is more prevalent (Davidson et al., 2008; Verchot et al., 2000).

Our analysis of spatial, temporal and environmental trends in CH_4 fluxes across the elevation gradient suggest that soil redox is the principal control on CH_4 flux, as is the

BGD
10, 17397–17438, 2013

case elsewhere in the tropics (Teh et al., 2005; Verchot et al., 2000; von Fischer and Hedin, 2007). CH_4 emissions were greatest from elevations, landforms or during times of year when soils were at their most sub-oxic. This conclusion is further supported by the strong inverse correlation observed between soil O_2 concentration (i.e. a proxy for soil redox potential) and CH_4 flux (Silver et al., 1999; Teh et al., 2005), with progressive declines in soil O_2 linked to increasingly large net CH_4 emissions (Fig. 3). Moreover, multiple regression models that included soil O_2, soil moisture and temperature indicated that soil O_2 concentration was the single best predictor of CH_4 flux, typically accounting for > 99 % of the variance in the entire dataset.

4.2 Andean ecosystems as atmospheric sources of N_2O

Ecosystems across the Kosñipata Valley were net sources of atmospheric N_2O. Fluxes progressively declined with elevation, with lower elevation habitats emitting substantially greater amounts of N_2O (premontane forest: $2.23 \pm 1.31\,kg\,N_2O-N\,ha^{-1}\,yr^{-1}$; lower montane forest: $1.68 \pm 0.44\,kg\,N_2O-N\,ha^{-1}\,yr^{-1}$) than higher elevation ones (upper montane forest: $0.44 \pm 0.47\,kg\,N_2O-N\,ha^{-1}\,yr^{-1}$; puna: $0.15 \pm 1.10\,kg\,N_2O-N\,ha^{-1}\,yr^{-1}$). Fluxes from lower elevation habitats exceeded the predictions for bottom-up emissions inventories for the region (< 0.5–$1.0\,kg\,N_2O-N\,ha^{-1}\,yr^{-1}$) (Werner et al., 2007) and were also substantially greater than fluxes observed in Ecuador (mean annual flux of $0.31 \pm 0.12\,kg\,N_2O-N\,ha^{-1}\,yr^{-1}$; range of -0.05–$1.27\,kg\,N_2O-N\,ha^{-1}\,yr^{-1}$) (Wolf et al., 2011). Although the cause for this divergence between these observations and past studies is unclear, it may be linked to the higher N status of lower elevation soils in the Kosñipata Valley, which tend to be more N-rich than soils in Ecuador (Wolf et al., 2011; Fisher et al., 2013, van de Weg et al., 2009).

Analysis of the field and laboratory data suggests that controls on N_2O fluxes in the Kosñipata Valley are complex and not easily reducible to simple predictive metrics. However, holistic examination of these combined datasets suggests that the availability of N, particularly NO_3^-, may play a pivotal role in limiting N_2O emissions across the

BGD
10, 17397–17438, 2013

elevation gradient. The central role of N availability in regulating N_2O fluxes is highlighted by the altitudinal trends in N_2O fluxes, available NO_3^- concentrations, potential N_2O and N_2 production, and ^{15}N-N_2O yields. Even though potential denitrification rates were similar across the elevation gradient (with the exception of upper montane forest), net N_2O fluxes and NO_3^- availability declined with elevation. Taken together, these data collectively suggest that altitudinal trends in N_2O fluxes were due to variations in denitrification, driven by differences in NO_3^- availability. Data on denitrification potential in upper montane forest further reinforces this interpretation of the data; upper montane forests had lower N_2O production potential, higher N_2 production potential and lower N_2O yields than other sites – all characteristics reflective of NO_3^--limitation of denitrification (Blackmer and Bremner, 1978; Weier et al., 1993; Yang et al., 2011). These data are in broad agreement with findings from Ecuador, where N availability was inversely proportional to altitude and was found to be the dominant control on N_2O efflux (Wolf et al., 2011).

Soil moisture and WFPS appeared to play a minor role in modulating N_2O fluxes across the elevation gradient; a surprising finding given the prominent role played by WFPS in regulating N_2O fluxes elsewhere in the seasonally dry tropics (Davidson et al., 1993, 2000, 2008; Davidson and Verchot, 2000; Keller and Reiners, 1994). Variations in soil moisture content and WFPS only appeared to influence N_2O fluxes in lower montane forest only during the dry season; whereas these variables had no discernible impact on N_2O fluxes in other elevations or during other seasons. This suggests that soil moisture and WFPS were not limiting during the 13 month period of observation, and that other factors more strongly constrained N_2O fluxes in these other habitats.

Comprehensive inspection of the environmental data (including soil moisture, WFPS and available N) suggests that the nature of the constraints on N_2O production may differ for each elevation band. WFPS fell within a relatively narrow range for premontane forest, lower montane forest during the wet season, and puna. Given the complexity of drivers for N_2O production, this makes it difficult to identify the "signal" of WFPS relative to the background environmental "noise" (Davidson and Verchot, 2000; Groffman et al.,

BGD
10, 17397–17438, 2013

2009). This signal-to-noise problem is further compounded by the fact that WFPS for these habitats was also within the predicted range where WFPS no longer limits N_2O production from denitrification (i.e. 60–90 %); as a consequence, N_2O fluxes are no longer increasing linearly with WFPS and have effectively reached saturation (Davidson, 1991; Davidson and Verchot, 2000). In addition, for puna, low NO_3^- availability and periods of very high WFPS (> 90 %) may have favoured low N_2O production and complete denitrification to N_2 (Blackmer and Bremner, 1978; Davidson, 1991; Weier et al., 1993; Yang et al., 2011). In contrast, for upper montane forest, soil moisture montane forest, soil moisture and WFPS did in fact vary significantly between seasons (wet season: 68.6 ± 1.9 %; dry season: 41.2 ± 1.8 %), although the very low NO_3^- availability probably constrained denitrification rates.

4.3 Preliminary area-weighted flux estimates for the Kosñipata Valley

The high mean annual CH_4 emissions from puna (56.94 ± 7.81 kg CH_4 – C ha^{-1} yr^{-1}) and high mean annual N_2O fluxes from premontane and lower montane forests (2.22 ± 1.31 kg N_2O – N ha^{-1} yr^{-1} and 1.68 ± 0.44 kg N_2O – N ha^{-1} yr^{-1}, respectively) may mean that the Kosñipata Valley is a stronger source for CH_4 and N_2O than previously predicted by bottom-up emissions inventories for upland tropical ecosystems in the region. To explore this possibility, we performed simple area-weighted flux calculations to estimate the potential contribution of different habitats to regional CH_4 and N_2O exchange. While we acknowledge that this "back-of-the-envelope" approach is not sufficient to accurately upscale plot-level fluxes to the regional scale, we believe it is still useful as a means of producing first order approximations of the source or sink potential of the region for CH_4 and N_2O.

Using published surface area estimates for different elevation bands for the Kosñipata Valley (Feeley and Silman, 2010), we calculated the areal fractions for each elevation band, multiplying these values by the mean annual fluxes of CH_4 or N_2O for our study sites, in order to derive area-weighted flux estimates for each elevation band (Table 5). To estimate the regional atmospheric flux of CH_4 or N_2O (i.e. for

BGD
10, 17397–17438, 2013

the Kosñipata Valley as a whole), we added together the area-weighted fluxes from each elevation band (Table 5). This exercise produced mean annual flux estimates of $9.42 \pm 1.80\,kg\,CH_4 - C\,ha^{-1}\,yr^{-1}$ and $1.18 \pm 0.79\,kg\,N_2O - N\,ha^{-1}\,yr^{-1}$, respectively.

The positive sign of the area-weighted CH_4 flux implies that the region as whole is probably a net atmospheric CH_4 source, strongly influenced by the contribution of puna acting as a regional "hotspot" for CH_4. This speculation is supported by evidence from remote sensing studies showing elevated atmospheric CH_4 concentrations in the tropical Andes, implying the presence of strong regional sources, such as waterlogged, sub-oxic/anoxic puna or *páramo* grasslands, unaccounted for by past bottom-up emissions inventories (Wania et al., 2007; Bergamaschi et al., 2007). Likewise the estimated regional N_2O flux for the Kosñipata Valley exceeds both model predictions for the region (< 0.5–$1.0\,kg\,N_2O - N\,ha^{-1}\,yr^{-1}$) (Werner et al., 2007) and observations from comparable ecosystems in Ecuador (mean annual flux of $0.31 \pm 0.12\,kg\,N_2O - N\,ha^{-1}\,yr^{-1}$) (Wolf et al., 2011), probably influenced by the strong emissions from lower elevation bands, which account for ~54 % of overall land cover.

While these area-weighted flux estimates may only be a first approximation, they are significant because these calculations suggest that Andean ecosystems may behave differently than previously thought, and may be larger emission sources than predicted. These findings also highlight the need for more intensive modeling studies to upscale plot-level measurements to the regional scale in order to more thoroughly evaluate the importance of these ecosystems for regional atmospheric budgets.

5 Conclusions

These data suggest that tropical Andean ecosystems are potentially important contributors to regional atmospheric budgets of CH_4 and N_2O, and that these ecosystems need to be considered more fully in future efforts to model and upscale CH_4 and N_2O fluxes from the terrestrial tropics. Ecosystems across this tropical altitudinal gradient were both atmospheric sources and sinks of CH_4, challenging long-standing assump-

BGD
10, 17397–17438, 2013

tions from the literature that upland tropical ecosystems are only net atmospheric CH_4 sinks. Simple area-weighted flux calculations suggest that high CH_4 fluxes from emissions "hotspots" (e.g. montane grasslands) may make the region as a whole a net atmospheric CH_4 source. This inference is supported by top-down remote sensing data that indicates the existence of strong local CH_4 sources in the tropical Andes, leading to enhanced atmospheric CH_4 concentrations. CH_4 fluxes were modulated by redox dynamics, with the largest emissions arising from elevations, landforms or during time periods when soil O_2 availability was lowest. Ecosystems across this altitudinal gradient were also net atmospheric sources of N_2O, with the largest N_2O emissions originating from lower elevation habitats (premontane forest, lower montane forest). Simple area-weighted flux calculations suggest that this region is likely to be a stronger source of atmospheric N_2O than previously predicted by bottom-up emissions inventories. This is largely due to the fact that lower elevation habitats are relatively large emission sources, and account for a substantial fraction of total land area in the region (~54 %). Proximate controls on N_2O fluxes were complex and difficult to elucidate from field measurements alone, although comprehensive inspection of combined field and laboratory data indicate that NO_3^- availability is the principal constraint on N_2O efflux, while soil moisture and water-filled porosity played a secondary role in modulating emissions. Any current and future changes in N management or anthropogenic N deposition may cause shifts in net N_2O fluxes from these tropical montane ecosystems, further enhancing this emission source.

Acknowledgements. The authors would like to acknowledge the agencies that funded this research; the UK Natural Environment Research Council (NERC; joint grant references NE/H006583, NE/H007849 and NE/H006753) and the Norwegian Agency for Development Cooperation (Norad; via a sub-contract to Y. A. T. managed by the Amazon Conservation Association). P. S. is a Royal Society–Wolfson Research Merit Award holder and P. M. is supported by an Australian Research Council Fellowship (FT110100457). Javier Eduardo Silva Espejo, Walter Huaraca Huasco, Adan Julian Ccahuana and the ABIDA NGO provided critical fieldwork and logistical support. Angus Calder and Vicky Munro provided invaluable laboratory support. Victoria Oliver provided data on soil characteristics for Hacienda Villa Carmen. Thanks to Adrian

BGD
10, 17397–17438, 2013

Tejedor from the Amazon Conservation Association, who provided assistance with site access and selection at Hacienda Villa Carmen. Thanks are also owed to TCH for providing comments on an earlier draft of this manuscript. This publication is a contribution from the Scottish Alliance for Geoscience, Environment and Society (http://www.sages.ac.uk).

References

Baggs, E. M., Richter, M., Cadisch, G., and Hartwig, U. A.: Denitrification in grass swards is increased under elevated atmospheric CO_2, Soil Biol. Biochem., 35, 729–732, 2003.

Bateman, E. J. and Baggs, E. M.: Contributions of nitrification and denitrification to N_2O emissions from soils at different water-filled pore space, Biol. Fert. Soils, 41, 379–388, 2005.

Belyea, L. R. and Baird, A. J.: Beyond "The limits to peat bog growth": cross-scale feedback in peatland development, Ecol. Monogr., 76, 299–322, 2006.

Bergamaschi, P., Frankenberg, C., Meirink, J. F., Krol, M., Dentener, F., Wagner, T., Platt, U., Kaplan, J. O., Korner, S., Heimann, M., Dlugokencky, E. J., and Goede, A.: Satellite chartography of atmospheric methane from SCIAMACHYon board ENVISAT: 2. Evaluation based on inverse model simulations, J. Geophys. Res.-Atmos., 112, 1–26, doi:10.1029/2006JD007268, 2007.

Bergamaschi, P., Frankenberg, C., Meirink, J. F., Krol, M., Villani, M. G., Houweling, S., Dentener, F., Dlugokencky, E. J., Miller, J. B., Gatti, L. V., Engel, A., and Levin, I.: Inverse modeling of global and regional CH_4 emissions using SCIAMACHY satellite retrievals, J. Geophys. Res.-Atmos., 114, 1–28, doi:10.1029/2009JD012287, 2009.

Blackmer, A. M. and Bremner, J. M.: Inhibitory effect of nitrate on reduction of N_2O to N_2 by soil microorganisms, Soil Biol. Biochem., 10, 187–191, 1978.

Breuer, L., Papen, H., and Butterbach-Bahl, K.: N_2O emission from tropical forest soils of Australia, J. Geophys. Res.-Atmos., 105, 26353–26367, 2000.

Davidson, E. A.: Fluxes of nitrous oxide and nitric oxide from terrestrial ecosystems, in: Microbial Production and Consumption of Greenhouse Gases: Methane, Nitrogen Oxides, and Halomethanes, edited by: Whitman, J. E. R. A. W. B., American Society of Microbiology, Washington, D.C., USA, 219–235, 1991.

BGD
10, 17397–17438, 2013

Davidson, E. A. and Verchot, L. V.: Testing the Hole-in-the-Pipe Model of nitric and nitrous oxide emissions from soils using the TRAGNET Database, Global Biogeochem. Cy., 14, 1035–1043, 2000.

Davidson, E. A., Matson, P. A., Vitousek, P. M., Riley, R., Dunkin, K., Garciamendez, G., and Maass, J. M.: Processes regulating soil emissions of NO and N_2O in a seasonally dry tropical forest, Ecology, 74, 130–139, 1993.

Davidson, E. A., Verchot, L. V., Cattanio, J. H., Ackerman, I. L., and Carvalho, J. E. M.: Effects of soil water content on soil respiration in forests and cattle pastures of eastern Amazonia, Biogeochemistry, 48, 53–69, 2000.

Davidson, E. A., Nepstad, D. C., Ishida, F. Y., and Brando, P. M.: Effects of an experimental drought and recovery on soil emissions of carbon dioxide, methane, nitrous oxide, and nitric oxide in a moist tropical forest, Glob. Change Biol., 14, 2582–2590, 2008.

Dutaur, L. and Verchot, L. V.: A global inventory of the soil CH(4) sink, Global Biogeochem. Cy., 21, 1–9, doi:10.1029/2006GB002734, 2007.

Eva, H. D., Belward, A. S., De Miranda, E. E., Di Bella, C. M., Gond, V., Huber, O., Jones, S., Sgrenzaroli, M., and Fritz, S.: A land cover map of South America, Glob. Change Biol., 10, 731–744, 2004.

Feeley, K. J. and Silman, M. R.: Land-use and climate change effects on population size and extinction risk of Andean plants, Glob. Change Biol., 16, 3215–3222, 2010.

Firestone, M. K. and Davidson, E. A.: Microbiological basis of NO and N2O production and consumption in soil, in: Exchange of trace gases between terrestrial ecosystems and the atmosphere, edited by: Andreae, M. O. and Schimel, D. S., 7–21, John Wiley & Sons, New York, 1989.

Fisher, J. B., Malhi, Y., Torres, I. C., Metcalfe, D. B., Van De Weg, M. J., Meir, P., Silva-Espejo, J. E., and Huasco, W. H.: Nutrient limitation in rainforests and cloud forests along a 3,000 m elevation gradient in the Peruvian Andes, Oecologia, 172, 889–902, 2013.

Fletcher, S. E. M., Tans, P. P., Bruhwiler, L. M., Miller, J. B., and Heimann, M.: CH_4 sources estimated from atmospheric observations of CH_4 and its C-13/C-12 isotopic ratios: 1. Inverse modeling of source processes, Global Biogeochem. Cy., 18, 1–17, doi:10.1029/2004GB002223, 2004a.

Fletcher, S. E. M., Tans, P. P., Bruhwiler, L. M., Miller, J. B., and Heimann, M.: CH_4 sources estimated from atmospheric observations of CH_4 and its C-13/C-12 isotopic ratios: 2. In-

BGD
10, 17397–17438, 2013

verse modeling of CH_4 fluxes from geographical regions, Global Biogeochem. Cy., 18, 1–15, doi:10.1029/2004GB002224, 2004b.
Frankenberg, C., Meirink, J. F., Van Weele, M., Platt, U., and Wagner, T.: Assessing methane emissions from global space-borne observations, Science, 308, 1010–1014, 2005.
Frankenberg, C., Bergamaschi, P., Butz, A., Houweling, S., Meirink, J. F., Notholt, J., Petersen, A. K., Schrijver, H., Warneke, T., and Aben, I.: Tropical methane emissions: a revised view from SCIAMACHY onboard ENVISAT, Geophys. Res. Lett., 35, 1–5, doi:10.1029/2008GL034300, 2008.
Fung, I., John, J., Lerner, J., Matthews, E., Prather, M., Steele, L., and Fraser, P.: Three-dimensional model synthesis of the global methane cycle, J. Geophys. Res.-Atmos., 96, 13033–13065, 1991.
Gauci, V., Gowing, D. J. G., Hornibrook, E. R. C., Davis, J. M., and Dise, N. B.: Woody stem methane emission in mature wetland alder trees, Atmos. Environ., 44, 2157–2160, 2010.
Gibbon, A., Silman, M. R., Malhi, Y., Fisher, J. B., Meir, P., Zimmermann, M., Dargie, G. C., Farfan, W. R., and Garcia, K. C.: Ecosystem carbon storage across the grassland–forest transition in the High Andes of Manu National Park, Peru, Ecosystems, 13, 1097–1111, 2010.
Girardin, C. A. J., Malhi, Y., Aragao, L., Mamani, M., Huasco, W. H., Durand, L., Feeley, K. J., Rapp, J., Silva-Espejo, J. E., Silman, M., Salinas, N., and Whittaker, R. J.: Net primary productivity allocation and cycling of carbon along a tropical forest elevational transect in the Peruvian Andes, Glob. Change Biol., 16, 3176–3192, 2010.
Groffman, P. M., Butterbach-Bahl, K., Fulweiler, R. W., Gold, A. J., Morse, J. L., Stander, E. K., Tague, C., Tonitto, C., and Vidon, P.: Challenges to incorporating spatially and temporally explicit phenomena (hotspots and hot moments) in denitrification models, Biogeochemistry, 93, 49–77, 2009.
Hall, S. J. and Matson, P. A.: Nitrogen oxide emissions after nitrogen additions in tropical forests, Nature, 400, 152–155, 1999.
Hirsch, A. I., Michalak, A. M., Bruhwiler, L. M., Peters, W., Dlugokencky, E. J., and Tans, P. P.: Inverse modeling estimates of the global nitrous oxide surface flux from 1998–2001, Global Biogeochem. Cy., 20, 1–17, doi:10.1029/2004GB002443, 2006.
Huang, J., Golombek, A., Prinn, R., Weiss, R., Fraser, P., Simmonds, P., Dlugokencky, E. J., Hall, B., Elkins, J., Steele, P., Langenfelds, R., Krummel, P., Dutton, G., and Porter, L.: Estimation of regional emissions of nitrous oxide from 1997 to 2005 using multinetwork mea-

BGD
10, 17397–17438, 2013

surements, a chemical transport model, and an inverse method, J. Geophys. Res.-Atmos., 113, 1–19, doi:10.1029/2007JD009381, 2008.
Keller, M. and Reiners, W. A.: Soil atmosphere exchange of nitrous-oxide, nitric-oxide, and methane under secondary succession of pasture to forest in the Atlantic lowlands of Costa-Rica, Global Biogeochem. Cy., 8, 399–409, 1994.
Keller, M., Kaplan, W. A., and Wofsy, S. C.: Emissions of N_2O, CH_4 and CO_2 from tropical forest soils, J. Geophys. Res.-Atmos., 91, 1791–1802, 1986.
Keller, M., Veldkamp, E., Weltz, A., and Reiners, W.: Effect of pasture age on soil trace-gas emissions from a deforested area of Costa Rica, Nature, 365, 244–246, 1993.
Kort, E. A., Patra, P. K., Ishijima, K., Daube, B. C., Jimenez, R., Elkins, J., Hurst, D., Moore, F. L., Sweeney, C., and Wofsy, S. C.: Tropospheric distribution and variability of N_2O: evidence for strong tropical emissions, Geophys. Res. Lett., 38, 1–5, doi:10.1029/2011GL047612, 2011.
Livingston, G. and Hutchinson, G.: Chapter 2: Enclosure-based measurement of trace gas exchange: applications and sources of error, in: Biogenic Trace Gases: Measuring Emissions from Soil and Water, edited by: Matson, P. and Harriss, R. C., Blackwell Science Ltd., Cambridge, MA, USA, 14–51, 1995.
Malhi, Y., Silman, M., Salinas, N., Bush, M., Meir, P., and Saatchi, S.: Introduction: elevation gradients in the tropics: laboratories for ecosystem ecology and global change research, Glob. Change Biol., 16, 3171–3175, 2010.
Melack, J. M., Hess, L. L., Gastil, M., Forsberg, B. R., Hamilton, S. K., Lima, I. B. T., and Novo, E.: Regionalization of methane emissions in the Amazon Basin with microwave remote sensing, Glob. Change Biol., 10, 530–544, 2004.
Nevison, C. D., Dlugokencky, E., Dutton, G., Elkins, J. W., Fraser, P., Hall, B., Krummel, P. B., Langenfelds, R. L., O'Doherty, S., Prinn, R. G., Steele, L. P., and Weiss, R. F.: Exploring causes of interannual variability in the seasonal cycles of tropospheric nitrous oxide, Atmos. Chem. Phys., 11, 3713–3730, doi:10.5194/acp-11-3713-2011, 2011.
Nevison, C. D., Mahowald, N. M., Weiss, R. F., and Prinn, R. G.: Interannual and seasonal variability in atmospheric N_2O, Global Biogeochem. Cy., 21, 1–13, doi:10.1029/2006GB002755, 2007.
Pedersen, A. R., Petersen, S. O., and Schelde, K.: A comprehensive approach to soil–atmosphere trace-gas flux estimation with static chambers, Eur. J. Soil Sci., 61, 888–902, 2010.

BGD
10, 17397–17438, 2013

Potter, C. S., Davidson, E. A., and Verchot, L. V.: Estimation of global biogeochemical controls and seasonality in soil methane consumption, Chemosphere, 32, 2219–2246, 1996.
Pumpanen, J., Kolari, P., Ilvesniemi, H., Minkkinen, K., Vesala, T., Niinisto, S., Lohila, A., Larmola, T., Morero, M., Pihlatie, M., Janssens, I., Yuste, J. C., Grunzweig, J. M., Reth, S., Subke, J. A., Savage, K., Kutsch, W., Ostreng, G., Ziegler, W., Anthoni, P., Lindroth, A., and Hari, P.: Comparison of different chamber techniques for measuring soil CO_2 efflux, Agr. Forest Meteorol., 123, 159–176, 2004.
Purbopuspito, J., Veldkamp, E., Brumme, R., and Murdiyarso, D.: Trace gas fluxes and nitrogen cycling along an elevation sequence of tropical montane forests in Central Sulawesi, Indonesia, Global Biogeochem. Cy., 20, 1–11, doi:10.1029/2005GB002516, 2006.
R Core Team: A Language and Environment for Statistical Computing, Online, Vienna, Austria: R Foundation for Statistical Computing, available at: http://www.R-project.org/, 2012.
Ridgwell, A. J., Marshall, S. J., and Gregson, K.: Consumption of atmospheric methane by soils: a process-based model, Global Biogeochem. Cy., 13, 59–70, 1999.
Silver, W., Lugo, A., and Keller, M.: Soil oxygen availability and biogeochemistry along rainfall and topographic gradients in upland wet tropical forest soils, Biogeochemistry, 44, 301–328, 1999.
Silver, W. L., Herman, D. J., and Firestone, M. K. S.: Dissimilatory nitrate reduction to ammonium in upland tropical forest soils, Ecology, 82, 2410–2416, 2001.
Spahni, R., Wania, R., Neef, L., van Weele, M., Pison, I., Bousquet, P., Frankenberg, C., Foster, P. N., Joos, F., Prentice, I. C., and van Velthoven, P.: Constraining global methane emissions and uptake by ecosystems, Biogeosciences, 8, 1643–1665, doi:10.5194/bg-8-1643-2011, 2011.
Teh, Y. A., Silver, W., and Conrad, M.: Oxygen effects on methane production and oxidation in humid tropical forest soils, Glob. Change Biol., 11, 1283–1297, doi:10.1111/j.1365-2486.2005.00983, 2005.
Teh, Y. A., Silver, W. L., Sonnentag, O., Detto, M., Kelly, M., and Baldocchi, D. D.: Large greenhouse gas emissions from a temperate peatland pasture, Ecosystems, 14, 311–325, 2011.
Templer, P. H., Lovett, G. M., Weathers, K. C., Findlay, S. E., and Dawson, T. E.: Influence of tree species on forest nitrogen retention in the Catskill Mountains, New York, USA, Ecosystems, 8, 1–16, 2005.

BGD
10, 17397–17438, 2013

Terazawa, K., Ishizuka, S., Sakatac, T., Yamada, K., and Takahashi, M.: Methane emissions from stems of *Fraxinus mandshurica* var. *japonica* trees in a floodplain forest, Soil Biol. Biochem., 39, 2689–2692, 2007.

Van De Weg, M. J., Meir, P., Grace, J., and Atkin, O. K.: Altitudinal variation in leaf mass per unit area, leaf tissue density and foliar nitrogen and phosphorus content along an Amazon–Andes gradient in Peru, Plant Ecol. Divers., 2, 243–254, doi:10.1080/17550870903518045, 2009.

Varner, R. K., Keller, M., Robertson, J. R., Dias, J. D., Silva, H., Crill, P. M., Mcgroddy, M., and Silver, W. L.: Experimentally induced root mortality increased nitrous oxide emission from tropical forest soils, Geophys. Res. Lett., 30, 1–4, doi:10.1029/2002GL016164, 2003.

Veldkamp, E., Purbopuspito, J., Corre, M. D., Brumme, R., and Murdiyarso, D.: Land use change effects on trace gas fluxes in the forest margins of Central Sulawesi, Indonesia, J. Geophys. Res.-Biogeo., 113, 1–11, doi:10.1029/2007JG000522, 2008.

Verchot, L. V., Davidson, E. A., Cattanio, J. H., and Ackerman, I. L.: Land-use change and biogeochemical controls of methane fluxes in soils of eastern Amazonia, Ecosystems, 3, 41–56, 2000.

Von Fischer, J. and Hedin, L.: Separating methane production and consumption with a field-based isotope dilution technique, Global Biogeochem. Cy., 16, 1–13, doi:10.1029/2001GB001448, 2002.

Von Fischer, J. C. and Hedin, L. O.: Controls on soil methane fluxes: tests of biophysical mechanisms using stable isotope tracers, Global Biogeochem. Cy., 21, 1–9, doi:10.1029/2006GB002687, 2007.

Von Fischer, J. C., Rhew, R. C., Ames, G. M., Fosdick, B. K., and Von Fischer, P. E.: Vegetation height and other controls of spatial variability in methane emissions from the Arctic coastal tundra at Barrow, Alaska, J. Geophys. Res.-Biogeo., 115, 1–11, doi:10.1029/2009JG001283, 2010.

Waddington, J. M. and Roulet, N. T.: Atmosphere-wetland carbon exchanges: Scale dependency of CO_2 and CH_4 exchange on the developmental topography of a peatland, Global Biogeochem. Cy., 10, 233–245, 1996.

Wania, R., Jolleys, M., and Buytaert, W.: Methane emissions from the Andean Paramo – a previously neglected methane source?, iLEAPS Newsletter, 7, 58–59, 2007.

BGD
10, 17397–17438, 2013

Weier, K. L., Doran, J. W., Power, J. F., and Walters, D. T.: Denitrification and the dinitrogen nitrous-oxide ratio as affected by soil-water, available carbon, and nitrate, Soil Sci. Soc. Am. J., 57, 66–72 1993. 1993.

Werner, C., Butterbach-Bahl, K., Haas, E., Hickler, T., and Kiese, R.: A global inventory of N_2O emissions from tropical rainforest soils using a detailed biogeochemical model, Global Biogeochem. Cy., 21, 1–18, doi:10.1029/2006GB002909, 2007.

Wolf, K., Veldkamp, E., Homeier, J., and Martinson, G. O.: Nitrogen availability links forest productivity, soil nitrous oxide and nitric oxide fluxes of a tropical montane forest in southern Ecuador, Global Biogeochem. Cy., 25, 1–12, doi:10.1029/2010GB003876, 2011.

Wolf, K., Flessa, H., and Veldkamp, E.: Atmospheric methane uptake by tropical montane forest soils and the contribution of organic layers, Biogeochemistry, 111, 469–483, 2012.

Yang, W. H., Teh, Y. A., and Silver, W. L.: A test of a field-based ^{15}N-nitrous oxide pool dilution technique to measure gross N_2O production in soil, Glob. Change Biol., 17, 3577–3588, 2011.

Zimmermann, M., Meir, P., Bird, M. I., Malhi, Y., and Ccahuana, A. J. Q.: Climate dependence of heterotrophic soil respiration from a soil-translocation experiment along a 3000 m tropical forest altitudinal gradient, Eur. J. Soil Sci., 60, 895–906, 2009.

Zimmermann, M., Meir, P., Bird, M. I., Malhi, Y., and Ccahuana, A. J. Q.: Temporal variation and climate dependence of soil respiration and its components along a 3000 m altitudinal tropical forest gradient, Global Biogeochem. Cy., 24, 1–13, doi:10.1029/2010GB003787, 2010a.

Zimmermann, M., Meir, P., Silman, M. R., Fedders, A., Gibbon, A., Malhi, Y., Urrego, D. H., Bush, M. B., Feeley, K. J., Garcia, K. C., Dargie, G. C., Farfan, W. R., Goetz, B. P., Johnson, W. T., Kline, K. M., Modi, A. T., Rurau, N. M. Q., Staudt, B. T., and Zamora, F.: No differences in soil carbon stocks across the tree line in the Peruvian Andes, Ecosystems, 13, 62–74, 2010b.

BGD
10, 17397–17438, 2013

Table 1. Site characteristics.

Elevation band (m a.s.l.)	Habitat	Areal coverage in the Kosñipata Valley (km^2)	Site name	Latitude (S)	Longitude (W)	Mean annual temperature (°C)	Mean annual precipitation (mm)	Soil C/N (0–10 cm depth)	Mesotopes	Plots	Flux chambers
600–1200	Premontane forest	7334	Hacienda Villa Carmen	12°53′43″	71°24′04″	23.4	5318	15	ridge, slope, flat	3	15
1200–2200	Lower montane forest	8923	San Pedro	13°2′56″	71°32′13″	18.8	2631	15	ridge, slope, flat	3	15
2200–3200	Upper montane forest	8066	Wayqecha	13°11′24″	71°35′13″	12.5	1706	25	slope, flat	3	15
3200–3700	Montane grasslands (puna)	5859	Tres Cruces	13°07′19″	71°36′54″	11.8	2200	14	ridge, slope, flat, basin	4	20

BGD
10, 17397–17438, 2013

Table 2. Summary of soil sampling scheme for denitrification potential experiment.

Elevation band (m.a.s.l.)	Habitat	Soil samples	Incubations	Rooting zone depth (cm)	Soil sample depth (cm)
600–1200	Premontane forest	11	19	0–10	5–10
1200–2200	Lower montane forest	2	3	0–15	20–25
2200–3200	Upper montane forest	3	5	0–25	20–25
3200–3700	Montane grasslands (puna)	6	10	0–10	5–10

BGD
10, 17397–17438, 2013

Table 3. Abiotic environmental variables for each elevation band for the wet and dry season. Upper case letters indicate differences among elevation bands and lower case letters indicate difference among seasons within elevation bands (Fisher's LSD, $P < 0.05$). Values reported here are means and standard errors.

Elevation Band (m.a.s.l.)	Habitat	Volumteric soil moisture (%)		Water-filled pore space (%)		Soil oxygen (%)	
	Wet season	Dry season	Wet season	Dry season	Wet season	Dry season	
600–1200	Premontane forest	39.3 ± 2.4 A a	42.9 ± 1.6 A a	65.6 ± 4.1 A a	71.5 ± 2.7 A a	NA	18.8 ± 0.3 A B
1200–2200	Lower montane forest	37.2 ± 1.0 A a	31.8 ± 1.5 B b	62.0 ± 1.6 A a	53.0 ± 1.7 B b	19.4 ± 0.1 A a	19.0 ± 0.1 A b
2200–3200	Upper montane forest	37.7 ± 1.0 A a	22.7 ± 1.0 C b	68.6 ± 1.9 A a	41.2 ± 1.8 C b	18.4 ± 0.2 A a	18.5 ± 0.1 B a
3200–3700	Montane grasslands (puna)	71.6 ± 0.5 B a	71.2 ± 0.5 D a	95.5 ± 0.2 B a	92.9 ± 0.7 D b	13.3 ± 0.4 B a	18.4 ± 0.1 B b

Elevation Band (m.a.s.l.)	Habitat	Soil temperature (°C)		Air temperature (°C)	
	Wet season	Dry season	Wet season	Dry season	
600–1200	Premontane forest	21.6 ± 0.1 A a	21.0 ± 0.1 A a	23.3 ± 0.2 A a	23.4 ± 0.5 A a
1200–2200	Lower montane forest	18.3 ± 0.1 B a	17.7 ± 0.1 B b	18.5 ± 0.2 B a	17.8 ± 0.2 B b
2200–3200	Upper montane forest	12.0 ± 0.1 C a	11.6 ± 0.1 C b	12.7 ± 0.1 C a	13.2 ± 0.1 C b
3200–3700	Montane grasslands (puna)	10.2 ± 0.1 D a	9.7 ± 0.1 D b	11.3 ± 0.2 D a	12.5 ± 0.3 C b

BGD
10, 17397–17438, 2013

Table 4. Methane fluxes for each elevation band for the wet and dry season. Lower case letters indicate differences among seasons within elevation bands (Fisher's LSD, $P < 0.05$). Numbers reported here are means and standard errors.

Elevation band (m.a.s.l.)	Habitat	Methane flux ($mg\,CH_4 - C\,m^{-2}\,d^{-1}$)	
		Wet season	Dry season
600–1200	Premontane forest	0.51 ± 0.41 a	−0.32 ± 0.11 b
1200–2200	Lower montane forest	−0.49 ± 0.13 a	−0.84 ± 0.07 b
2200–3200	Upper montane forest	−0.54 ± 0.11 a	−1.22 ± 0.04 b
3200–3700	Montane grasslands (puna)	18.57 ± 2.55 a	0.97 ± 0.47 b

BGD
10, 17397–17438, 2013

Table 5. Preliminary area-weighted flux estimates for the Kosñipata Valley, Manu National Park, Peru. Surface areas and fractional areas calculated from data published in Feeley and Silman (2010). Flux values reported here are means and standard errors.

Elevation band (m.a.s.l.)	Habitat	Surface area (ha)	Fractional area	Unweighted mean annual fluxes		Area-weighted mean annual fluxes	
				CH_4 $kg\,CH_4 - C\,ha^{-1}\,yr^{-1}$	N_2O $kg\,N_2O - N\,ha^{-1}\,yr^{-1}$	CH_4 $kg\,CH_4 - C\,ha^{-1}\,yr^{-1}$	N_2O $kg\,N_2O - N\,ha^{-1}\,yr^{-1}$
600–1200	Premontane forest	733 428	0.24	−0.51 ± 0.47	2.23 ± 1.31	−0.14 ± 0.12	0.54 ± 0.32
1200–2200	Lower montane forest	892 338	0.30	−2.34 ± 0.29	1.68 ± 0.44	−0.69 ± 0.09	0.50 ± 0.13
2200–3200	Upper montane forest	806 588	0.27	−2.99 ± 0.29	0.44 ± 0.47	−0.80 ± 0.08	0.12 ± 0.13
3200–3700	Montane grasslands (puna)	585 883	0.19	56.94 ± 7.81	0.15 ± 1.10	11.05 ± 1.52	0.03 ± 0.21
TOTALS		3 018 236	1.00			9.42 ± 1.80	1.18 ± 0.79

BGD
10, 17397–17438, 2013

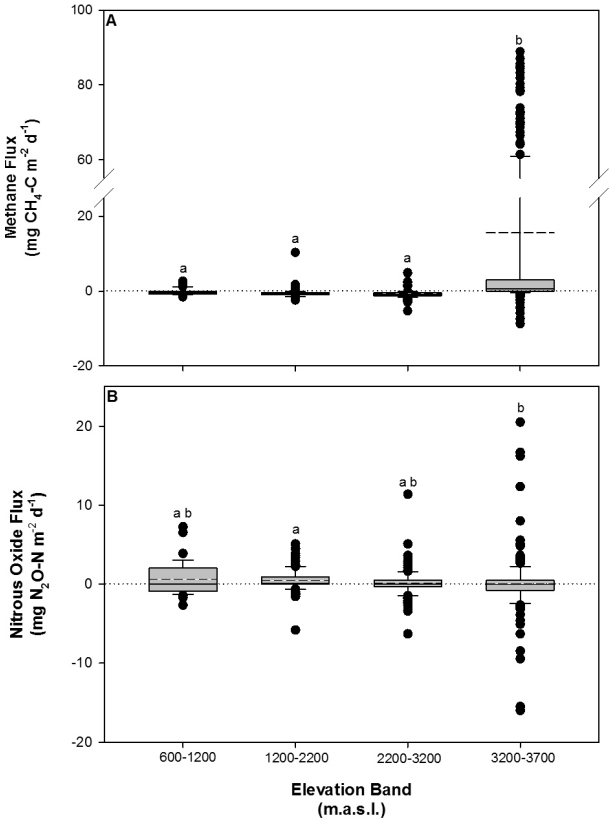

Fig. 1. (A) Net CH_4 and **(B)** net N_2O fluxes by elevation band. The short-dash line within each box represents the mean, whereas the solid line represents the median. Boxes enclose the interquartile range, whiskers indicate the 90th and 10th percentiles. The dotted line running across the boxes indicates zero net flux. Lower case letters indicate statistically significant differences among means (Fisher's LSD, $P < 0.05$).

BGD
10, 17397–17438, 2013

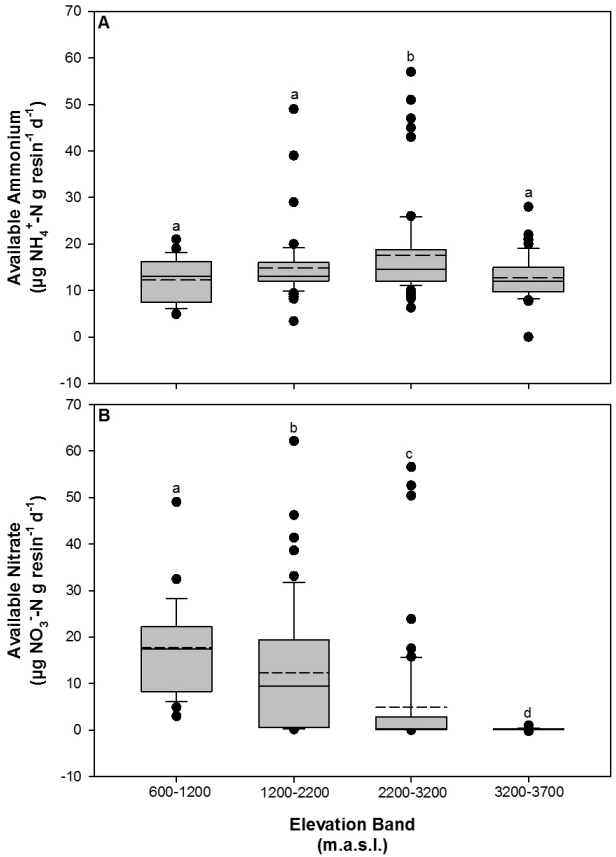

Fig. 2. (A) Available NH_4^+ and **(B)** available NO_3^- concentrations by elevation band. The short-dash line within each box represents the mean, whereas the solid line represents the median. Boxes enclose the interquartile range, whiskers indicate the 90th and 10th percentiles. Lower case letters indicate statistically significant differences among means (Fisher's LSD, $P < 0.05$).

BGD
10, 17397–17438, 2013

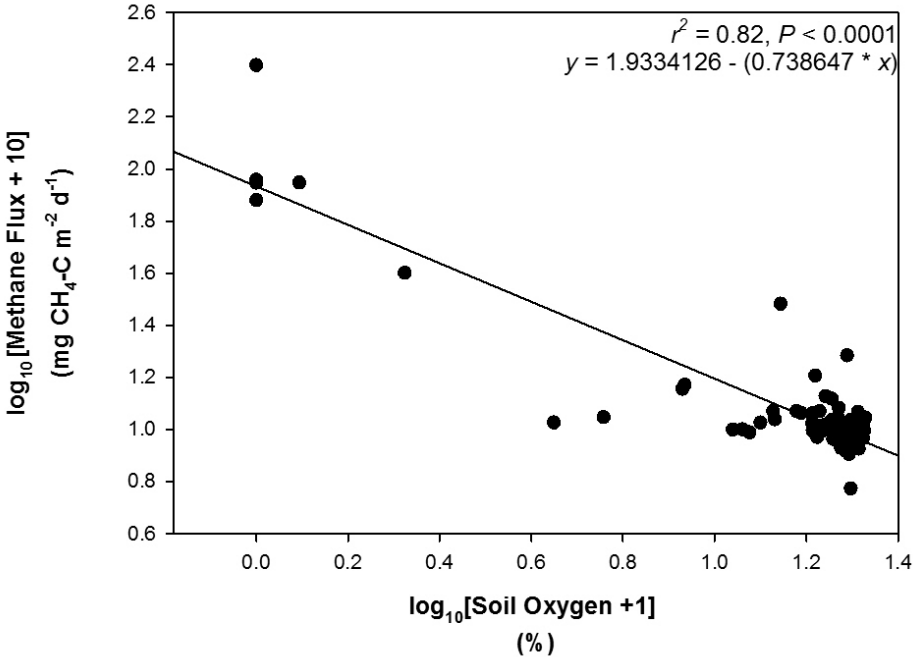

Fig. 3. Mean plot-level CH_4 flux against mean plot-level soil O_2 for the 0–10 soil depth. For CH_4 flux, 10 was added to the raw data so that negative or zero net fluxes could be log_{10}-transformed. For O_2, 1 was added to the raw data so that zero values could be log_{10}-transformed.

BGD
10, 17397–17438, 2013

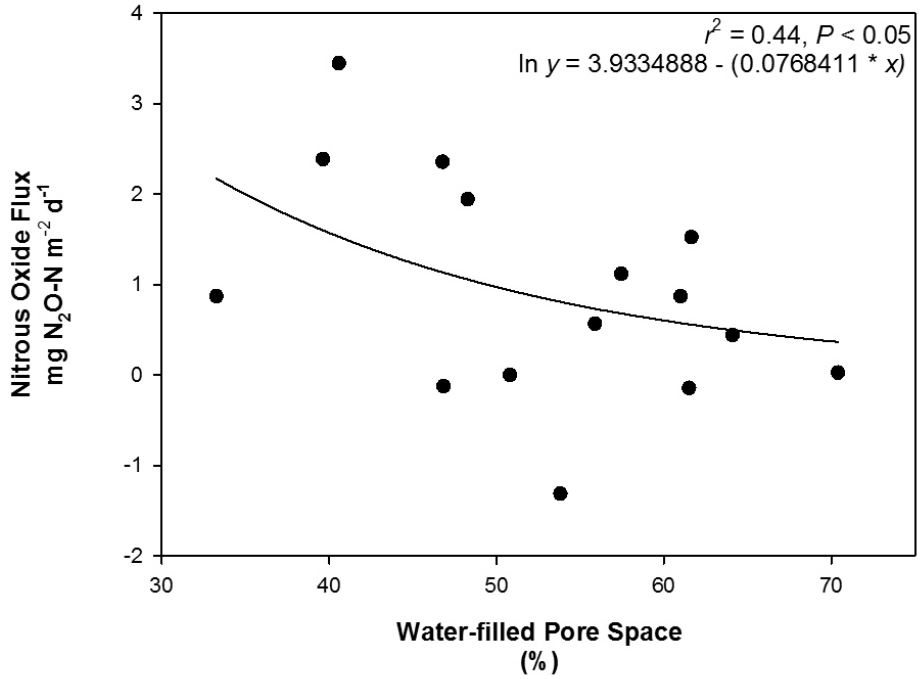

Fig. 4. Mean plot-level N_2O flux against mean plot-level water-filled pore space for lower montane forest during the dry season.

BGD
10, 17397–17438, 2013

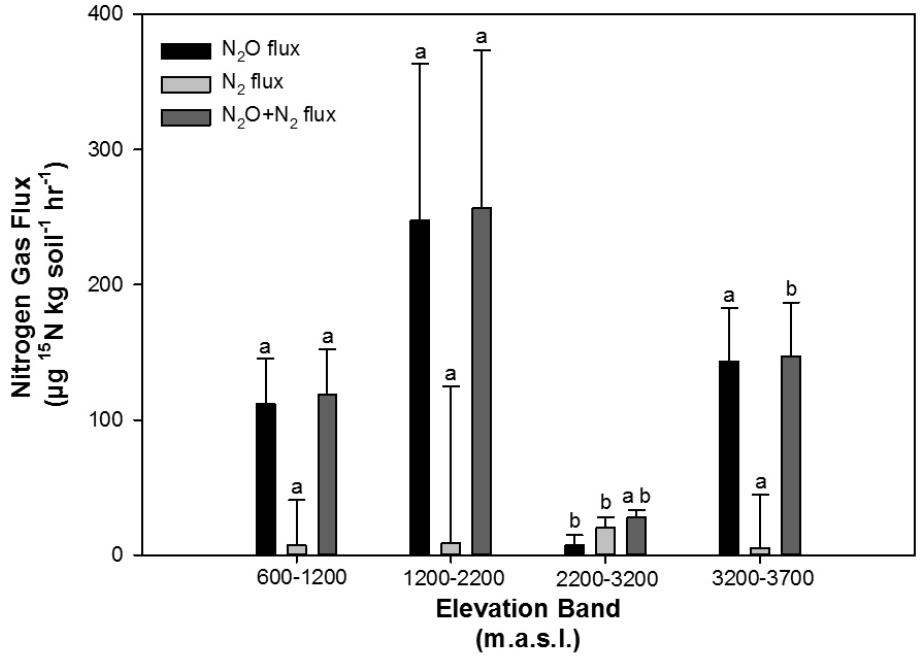

Fig. 5. Potential rates of N_2O production, N_2 production and total ($N_2O + N_2$) denitrification from $^{15}N\text{-}NO_3^-$ laboratory tracer studies. Lower case letters indicate statistically significant differences among $^{15}N\text{-}N_2O$, $^{15}N\text{-}N_2$ or total denitrification fluxes (Fisher's LSD, $P < 0.05$).

BGD
10, 17397–17438, 2013